Received: 26 December 2022 | Revised: 19 February 2023 | Accepted: 4 March 2023

DOI: 10.1002/jobm.202200718

RESEARCH PAPER

Journal of Basic Microbiology

Biogenic synthesized copper oxide nanoparticles by *Bacillus subtilis*: Investigating antibacterial activity on the *mexAB-oprM* efflux pump genes and cytotoxic effect on MCF-7 cells

Hossein Azizi[1] | **Neda Akbari**[1] | **Farnaz Kheirandish**[1,2,3] | **Asghar Sepahvand**[1,2]

[1]Department of Microbiology, Arak Branch, Islamic Azad University, Arak, Iran

[2]Department of Medical Parasitology and Mycology, Faculty of Medicine, Lorestan University of Medical Sciences, Khorramabad, Iran

[3]Department of Medical Biotechnology, Faculty of Medicine, Khorramabad, Iran

Correspondence
Neda Akbari, Department of Microbiology, Arak Branch, Islamic Azad University, Arak 1477893780, Iran.
Email: akbari.ne@gmail.com

Abstract

One of the main characteristics of *Pseudomonas aeruginosa* is remarkable intrinsic antibiotic resistance which is associated with production of β-lactamases and the expression of inducible efflux pumps. Nanoparticles (NPs) are a novel option for coping with this resistant bacteria. Hence, the aim of present study was production of CuO NPs via *Bacillus subtilis* and applied them to deal with resistant bacteria. For this purpose, first NPs were synthesized and were analyzed with different standard techniques containing scanning electron microscope, Fourier-transform infrared spectroscopy, and X-ray powder diffraction. Microdilution Broth Method and real-time polymerase chain reaction were used to antibacterial properties of the CuO NPs and expression of *mexAB-oprM* in clinical samples of *P. aeruginosa*, respectively. The cytotoxic effect of CuO NPs was also evaluated on MCF7 as a breast cancer cell line. Finally, the data were analyzed by one-way analysis of variance and Tukey's tests. The size of CuO NPs was in the range of 17–26 nm and showed antibacterial effect at <1000 μg/mL concentrations. Our evidence noted that the antibacterial effects of the CuO NPs occurred through the downregulation of *mexAB-oprM* and upregulation of *mexR*. The interesting point was that CuO NPs had an inhibitory effect on MCF7 cell lines with the optimal inhibition concentration at IC50 = 25.73 μg/mL. Therefore, CuO NPs can be considered as a promising medical candidate in the pharmaceutical industry.

KEYWORDS

copper oxide, cytotoxic effect, efflux pump, gene regulation, MDR, nanoparticle

Abbreviations: FTIR, Fourier-transform infrared spectroscopy; MIC, minimum inhibitory concentration; NPs, nanoparticles; SEM, field emission scanning electron microscopy; XRD, X-ray diffraction.

1 | INTRODUCTION

Green chemistry aids to decrease the application of hazardous substances and evaluate the efficiency of chemical processes [1, 2]. The use of microorganisms as a sustainable and readily available tool to produce Nanoparticles (NPs) has received much attention in recent years [3, 4]. NPs were considered due to their antibacterial properties based upon inherent inhibitory effects of particles and ample interactive surface [1, 5, 6]. NPs can be produced by microorganisms, especially bacteria as a defense and resistance mechanism in their natural environment [7], for instance, metallic NPs production for resistance to metallic ions [8, 9]. The bacterial cell wall has a negative electrical charge that leads to electrostatic interaction with positive metallic ions, and contains certain enzymes responsible for producing NPs. When the metallic ions are turned into NPs, they can pass through the cell wall due to their smaller size [8, 10]. Among different NPs, CuO is cheap, highly antibacterial, and stable with a longer half-life in comparison to the organic antimicrobial compounds [11, 12]. As CuO NPs attach to the cell membrane, they affect the permeability and cellular respiration disturbance [13]. The antibacterial abilities of CuO NPs are due to their abrasive nature. The jagged surface of these NPs mechanically damages the cell membrane [14]. Additionally, the released Cu^{2+} ions are attracted to the negatively charged carboxylic group of the cell wall lipoproteins as followed by the cell entry and enzyme function alterations, which inevitably lead to bacteria death [15, 16]. *Actinomycetes* and *Aliivibrio fischeri* can synthesize CuO NPs which inhibit the growth of a variety of bacteria [8, 17]. Bacteria have been subjected to evolutionary processes to develop antibiotic resistance, since the advent of antibiotic production and prescription of them. This has caused a notable reduction in the efficiency of antibiotics [18–20]. Among resistant bacteria, *Pseudomonas aeruginosa* is a primary cause of life-threatening nosocomial infections in immunocompromised patients and severe infection requiring ventilation, such as COVID-19. A number of new alternative drugs have been developed to treat antibiotic resistant *P. aeruginosa*, including NPs, antimicrobial peptides, quorum sensing inhibitors, bacteriophage therapy, and antimicrobial photodynamic therapy. Increased expression of MexAB-OprM efflux pumps is an important mechanism of antibiotic resistance in *P. aeruginosa*, and treatment with inhibitors of active efflux pumps appears to be an attractive strategy to combat its multidrug resistance (MDR) [21–23]. The expression of MexAB–OprM is regulated by *mexR* gene [24]. Iron oxide NPs has a fading effect on the *mexA* gene of *P. aeruginosa* [25]. Whereas after silver NPs application *mexB* was downregulated [26].

In this study, we have attempted to synthesize CuO NPs via the green methods, and subsequently measure the antibacterial effect after NPs verification via phenotypic and genotypic methods. Therefore, synthesized CuO NPs carried out as suitable markers for evaluating the activity and expression of *mexAB-oprM* genes and *mexR* regulator genes of efflux pump gene.

2 | MATERIALS AND METHODS

2.1 | Clinical isolates collection

Ten *P. aeruginosa* were collected from the clinical centers of Khorramabad city during 3 months in 2020. Bacterial specimens were collected from various clinical samples, such as blood, wounds, bronchial lavage, urine, etc. Then, all isolates were identified by biochemical tests [27]. A standard strain (accession: ATCC 25922) was bought from the Iranian biological resource center, and was used alongside the clinically derived *P. aeruginosa* as a control.

2.2 | Antibiotic sensitivity analysis

Samples were tested for antibiotic resistance by the Kirby-Bauer test. Different antibiotics family members were purchased from PADTAN TEB Company, based on the Clinical & Laboratory Standards Institute (CLSI) table [28]. The antibiotic disks included ceftriaxone 30 μg, imipenem 10 μg, cefepime 30 μg, amikacin 30 μg, cefazolin 30 μg, gentamicin 10 μg, ciprofloxacin 5 μg, minocycline 10 μg, meropenem 5 μg, clarithromycin 15 μg, and cotrimoxazole 25 μg. Eventually, we considered isolates as MDR which was resistant to at least one of the three antibiotic classes.

2.3 | NP biosynthesis

Bacillus subtilis (Accession: IBRC- M10742) was also bought from the Iranian biological resource center for NPs synthesis. Lyophilized *B. subtilis* was first inoculated into the Tryptic soy broth (TSB) for a short incubation period in 37°C to biosynthesize NPs, followed by streaking on blood agar medium. Colonies resulting from the mentioned cultures were used to inoculate Erlenmeyer flasks, containing TSB 250 mL for yielding bacterial culture supernatants. The pH was set to 7.2, and

the growth medium was incubated in a shaker incubator for 24–48 h. The culture medium was centrifuged at 10,000*g* for 15 min. In the next step, 10 mM copper sulfate [$CuSo_4 \cdot 5H_2O$] was added to 25 mL of supernatant with subsequent incubation in 100°C for 15 min. This caused the solution to turn brownish red from blue. To separate the NPs, centrifugation was done at 10,000*g* for 15 min. The pellet was washed many times with deionized-distilled water, and subsequently with ethanol to remove the blue molecules. Finally, the CuO NPs were heated and dried at 100°C [8].

2.4 | Evaluation and verification of biosynthesized NPs

Different techniques were employed to confirm NPs precipitation. Fourier-transform infrared spectroscopy (FTIR) was recorded using a Fourier transmission infrared spectrometer (Bruker) in the range of 400–4000 cm^{-1}. Crystalline phase detection of the NPs was done by the X-ray diffractometer (XRD) (D8 Advance from Bruker Model, manufactured by Germany) with Cu Kα radiations; $\lambda = 1.5406$ Å, at 35 kW, 35 mA current, and Bragg angles of $10 > 2\theta > 8$. NPs detection was done by scanning electron microscope (SEM) analysis; it demonstrates the particle size and shape. The pictures were taken and recorded.

2.5 | Evaluating the antibacterial properties of NPs using the microdilution broth method

Minimum inhibitory concentration (MIC) was determined by broth microdilution method in the sterile 96-well plates with the CLSI method. A 3000 μg/mL stock of the NPs was made with the sterile Mueller-Hinton broth containing 10% DMSO. In the following, 50 μL of the CuO NPs was added from the third to the twelfth plate row, and 100 μL was added to the first and second rows. Dilution was done in the wells from the second to the tenth row. A 24-h culture of *P. aeruginosa* at the 0.5 McFarland standard (1.5×10^8 CFU/mL) was added from the second till the tenth rows. The plates were incubated in 37°C and 50% humidity for 24–48 h. In the next step, 2, 3, 5-triphenyl-tetrazolium chloride at the concentration of 5 mg/mL was used as a visual marker of microorganism growth. The well concentration without color was reported as the MIC. The DMSO solvent at the concentration of 1% was used as a negative control. Gentamicin was used as a positive control. Each test was performed in triplicate [29].

2.6 | The effect of NP on the *mexAB-OprM* efflux pump gene expression

Real-time polymerase chain reaction (PCR) measured the effect of CuO NPs on the expression of *mexAB-oprM* efflux pump gene. In the current investigation, the expression of efflux genes such as *mexA*, *mexB*, and *oprM* were evaluated. Bacterial RNA extraction was done with GeneAll's RNA extraction kit (Korea) according to the manufacturer's instruction in identical conditions, and at the same time for treated and controlled bacteria *rpo-D* was used as an internal control. The concentration and quality of the RNA were evaluated with a Nanodrop device (Thermo Fisher Scientific 2000c). The complementary DNA (cDNA) synthesis was done according to the structure of AnaCell's kit. The cDNA quantity and quality were assessed by a Nanodrop device for treatment and control groups. The complementation specificities of real-time PCR primers were evaluated to determine the best annealing temperature. A SYBR green-containing PCR master mix produced by SMOBIO Technology was used to measure efflux pump gene expression. Total reaction volumes were fixed at 20 μL, including 1 μL of cDNA, 10 μL of SYBR green master mix, forward and reverse primers for *mexAB-oprM* (2 μL) and *mexR*. Diethyl pyrocarbonate (DEPC) treated water was used to adjust the volume. The real-time PCR was done with a CORBET device at Lorestan University of Medical Sciences. Initial denaturation was done at 95°C for 5 min, 40 cycles were denatured at 95°C for 15 s, the annealing temperature of each gene was set for 20 s, extension happened at 72°C for 20 s, the final extension was performed at 72°C for 45 s. The final step was 55–95°C for 15 s to acquire a melting curve. Primer sequences are shown in Table 1 [30].

2.7 | Effect of CuO NPs on MCF-7 cell line

The cytotoxic properties of CuO NPs were evaluated on MCF7 cell lines which were purchased from the Iranian Genetic Resources Center (IBRC). The cells were cultured in 5 ml of ready-made media control solution Dulbecco's modified Eagle's medium with fetal bovine serum 10% at 37°C. The effect of CuO NPs growth inhibition on MCF7 cells was assessed using a quantitative colorimetric 3-(4,5-dimethylthiazol-2-yl)−2,5-diphenyltetrazolium bromide (MTT) cytotoxicity test. The cytotoxic effect of taxol (Bristol Myers Squibb) was also investigated as a common chemotherapy drug. After 24 h incubation MCF7 cell lines were treated in triplet with concentrations of 1000, 500, 250, 125, 62.5, 31.25, and 0 (as negative control) μg/mL in 96-well plates. Then, they were incubated for 48 h. In the next step,

TABLE 1 Primers used in real-time polymerase chain reaction.

Target gene	Primer (5′–3′)	Product weight (bp)	T_m (°C)	Reference
mexA	F:5′-ACCTACGAGGCCGACTACCAGA-3′	179	64	[30]
	R: 5′-GTTGGTCACCAGGGCGCCTTC-3			
mexB	F: 5′-GTGTTCGGCTCGCAGTACTC-3′	244	60	[30]
	R: 5′-AACCGTCGGGATTGACCTTG-3′			
oprM	F: 5′-CCATGAGCCGCCAACTGTC-3′	205	60	[30]
	R: 5′-CCTGGAACGCCGTCTGGAT-3′			
mexR	F: 5′-GAACTACCCCGTGAATC-3′	411	59	[30]
	R: 5′-CACTGGTCGAGGAGATGC-3′			
rpo-D	F: 5′-ACCCGTGAA GGT GAA ATCAG-3′	672	60	[30]
	R: 5′-TTCAGCTGGAGCTTTAGCAAT-3′			

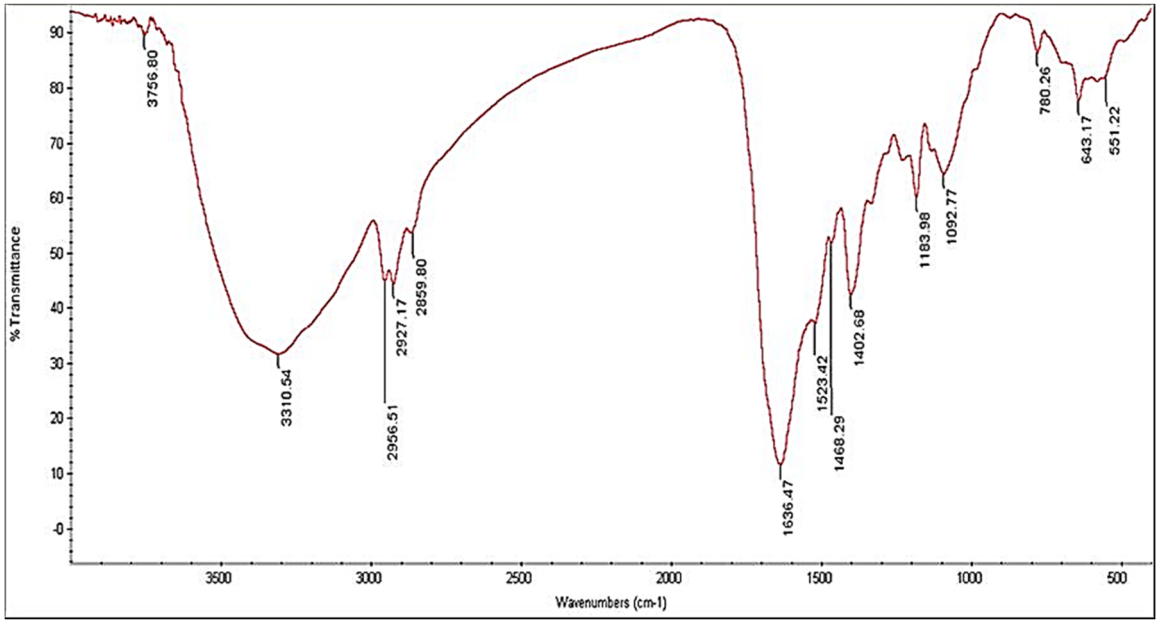

FIGURE 1 Fourier-transform infrared spectroscopy spectrum of biosynthesized CuO nanoparticles using *Bacillus subtilis*.

10 μL of MTT solution (5 mg/mL) was added. DMSO (100 μL) was added to each well to dissolve Formazan crystals, and the plates were placed at room temperature in darkness for 3–4 h. The optical density of each well was read at the wavelength between 492 and 630 nm using ELISA readers (Stat Fax 4700 Awareness Technology Inc.). All the tests were also performed in three replicates for Taxol [31].

2.8 | Statistical analysis

All the data were analyzed by one-way analysis of variance and Turkey's tests on SPSS software version 22. Statistical significance was considered $p < 0.05$.

3 | RESULTS

3.1 | NP biosynthesis assessments

3.1.1 | FTIR mediated assessment

The FTIR analysis was done to identify functional groups in the CuO NPs (Figure 1). The FTIR showed different chemical bonds formed CuO NPs. These functional groups were from *B. subtilis* secondary metabolites. FTIR analysis showed different peaks as described below; 551.22, 643.17, 780.22, 1092.77, 1183.98, 1402.68, 1468.29, 1523.42, 1636.47, 2859.80, 2971.17, 2956.51, 3310.54, and 3756.80 cm^{-1}. The FTIR

spectrum was measured in 400–4000 cm^{-1}. A strong peak of 3756.80 cm^{-1} was due to the presence of O–H groups in the phenol and alcohol peaks at 1636.47 cm^{-1} corresponded to C–C bonding in the aromatic rings. Peaks at 1092.77 cm^{-1} also corresponded to C–N bonds in the aliphatic amino acids. A strong peak at 780.22 cm^{-1} corresponded to =C–H groups in alkenes. According to the prior studies of Sivaraj et al., a peak at 551.22 cm^{-1} is related to the oxygen–metal/M–O bonding [32]. These functional groups lead to CuO NPs formation, which is responsible for protein and enzyme reduction. The FTIR spectrum of CuO NPs had vibrations at 400–4000 cm^{-1}, which supplied further validations for M–O (M=Cu) existence.

3.1.2 | XRD mediated evaluation

The substance crystal structure X-ray power diffraction was used to conduct further evaluations and determine the phases. The CuO NPs powder synthesized for XRD was scanned at a speed of 0.02° s^{-1} and 2θ. The pattern of CuO is variable from 20° till 80°. The CuO Bragg angle peak was seen at the level of −111. This is in accordance with the crystallography standard patterns of JCPD (accession 89-1117) and did not show any secondary phases. Figure 2 shows the strong and narrow observed peak is indicative of an appropriate NPs crystal structure.

3.1.3 | Morphology and size evaluation of NPs by SEM

SEM examinations were conducted to evaluate NPs size and morphology. Figure 3 shows CuO NPs biosynthesized by *B. subtilis*. As evident from the pictures, the CuO NPs are crystalized into a spherical shape with a diameter of 17–26 nm.

3.2 | The MICs of the CuO NPAgainst the *P. aeruginosa* isolates

The Kirby–Bauer antibiogram test showed that 100% isolates were resistant to different antibiotic families, so all of the isolates can be considered MDR. Results of the MIC test for the antibacterial effect of CuO NPs after three repetitions for each *P. aeruginosa* strain are presented in Table 2.

3.3 | *mexAB-oprM* and the *mexR* gene expression

The gene expression data resulting of *mexAB-oprM* and the *mexR* regulatory gene were turned into relative expression by the $2^{-\Delta\Delta C_t}$ formula from real-time PCR (Figure 4). According to our results, *mexR* gene was overexpressed after NPs treatment; as MexR is a down regulator of MexAB-OprM.

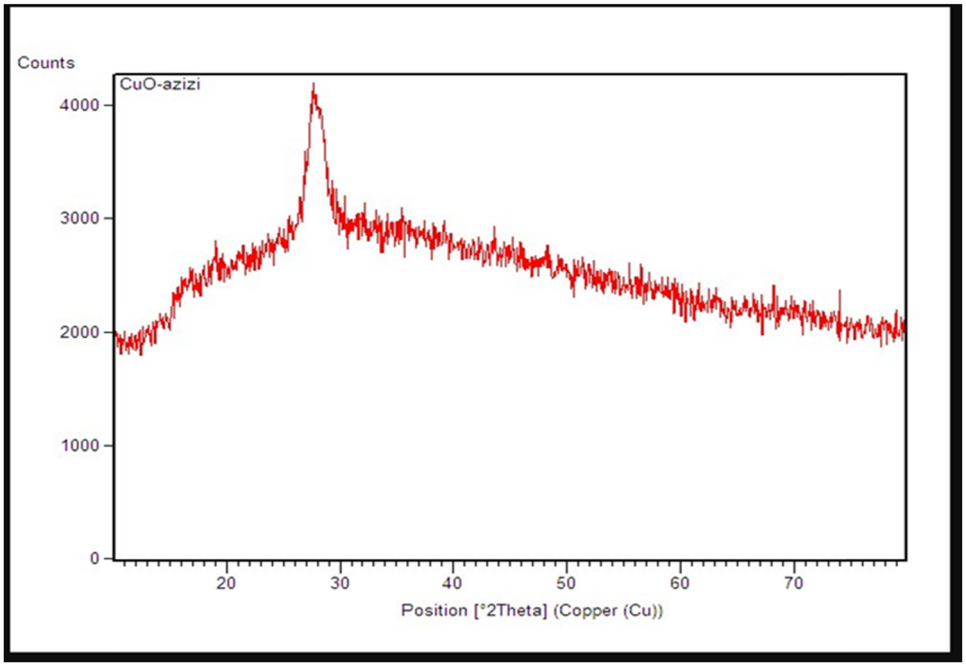

FIGURE 2 X-ray diffraction analysis of biosynthesized CuO nanoparticles using *Bacillus subtilis*.

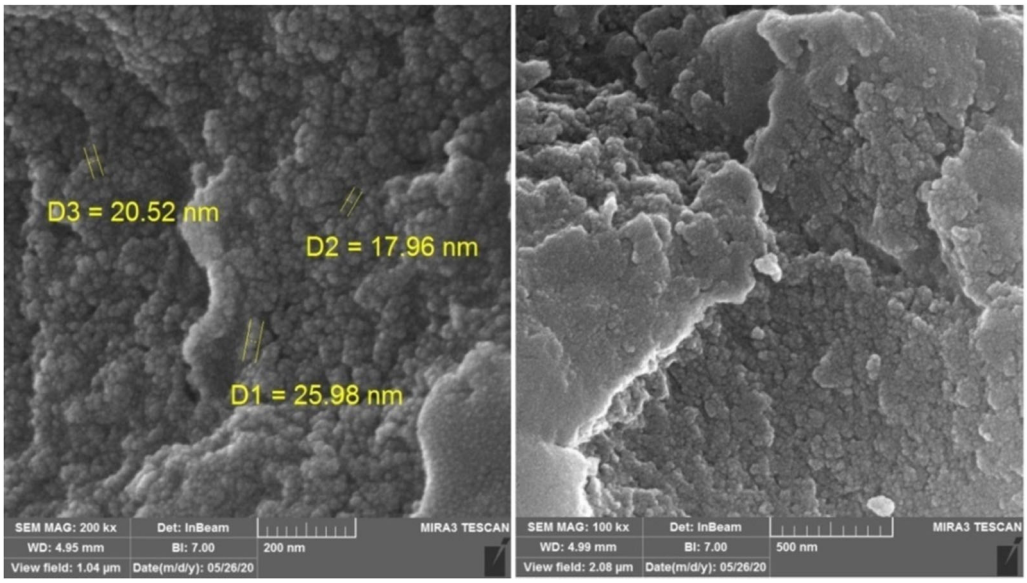

FIGURE 3 Scanning electron microscopy image of biosynthesized CuO nanoparticles using *Bacillus subtilis*.

TABLE 2 Evaluation of the inhibitory effect of synthesized CuO nanoparticles using *Bacillus subtilis*.

Pseudomonas aeruginosa strain	MIC test result (µg/mL)	Gentamycin control (µg/mL)
1	250	64
2	500	32
3	250	16
4	250	32
5	125	32
6	125	16
7	250	32
8	250	32
9	500	64
10	500	64
11	250	8

Abbreviation: MIC, minimum inhibitory concentration.

3.4 | Results of cytotoxicity of CuO NPs

The synthesized CuO NPs had a lethal activity against cancer cell lines in a dose-dependent manner with a straight correlation. Therefore, the lowest cytotoxicity of NPs at the concentration of 31.25 µg/mL was equal to 31.8%. The inhibitory concentration of 50% (IC50) was calculated 25.73 µg/mL at concentrations of 500 and 1000 µg/mL, the rate of growth inhibition for NPs and Taxol overlapped according to Figure 5, but at the lowest concentration of 31.25, Taxol was the strongest growth inhibitor for cancer cells (Table 3).

4 | DISCUSSION

In this study, CuO NPs were synthesized by *B. subtilis* which grows in stressful and rough environmental conditions. Besides that, *B. subtilis* has different properties such as rapid growth, production of biomass, production a lot of metabolites, high regenerative power of metals, resistance to environmental changes, short time to produce and extract NPs, and most importantly extracellular for the biosynthesis of CuO NPs [33]. The diameter of the synthesized NPs in this study was 17-26 nm, which is useful for nanobiotechnological applications. CuO NPs can penetrate into the bacterial cells due to their smaller size (nanometer) compared to the pore size of cell wall (micrometer) [34]. Shantkriti et al. biosynthesized the CuO NPs in *Pseudomonas fluorescens* with particle diameters of 20–80 nm [35]. Another study synthesized the CuO NPs by *Actinomycetes* at a particle diameter of 61.7 nm [8]. Eltarahony al. also biosynthesized the size of CuO NPs by *Proteus Mirabilis* with the size of 10 nm [36]. According to different studies, the size of produced CuO NPs can be various based on the host bacteria.

In the last decades, MDR of microbes have arisen due to excessive and irresponsible consumption of antimicrobial compounds [37, 38]. In this study, the resistance of isolates to various antibiotics was measured 100%. After CuO NPs synthesis, the antibacterial effects were evaluated by MIC test and demonstrated that the MICs for all *P. aeruginosa* were less than 1000 µg/mL, which showed the efficacy of CuO growth inhibition. Parallel to our results, Ehsan et al. reported inhibitory effects of

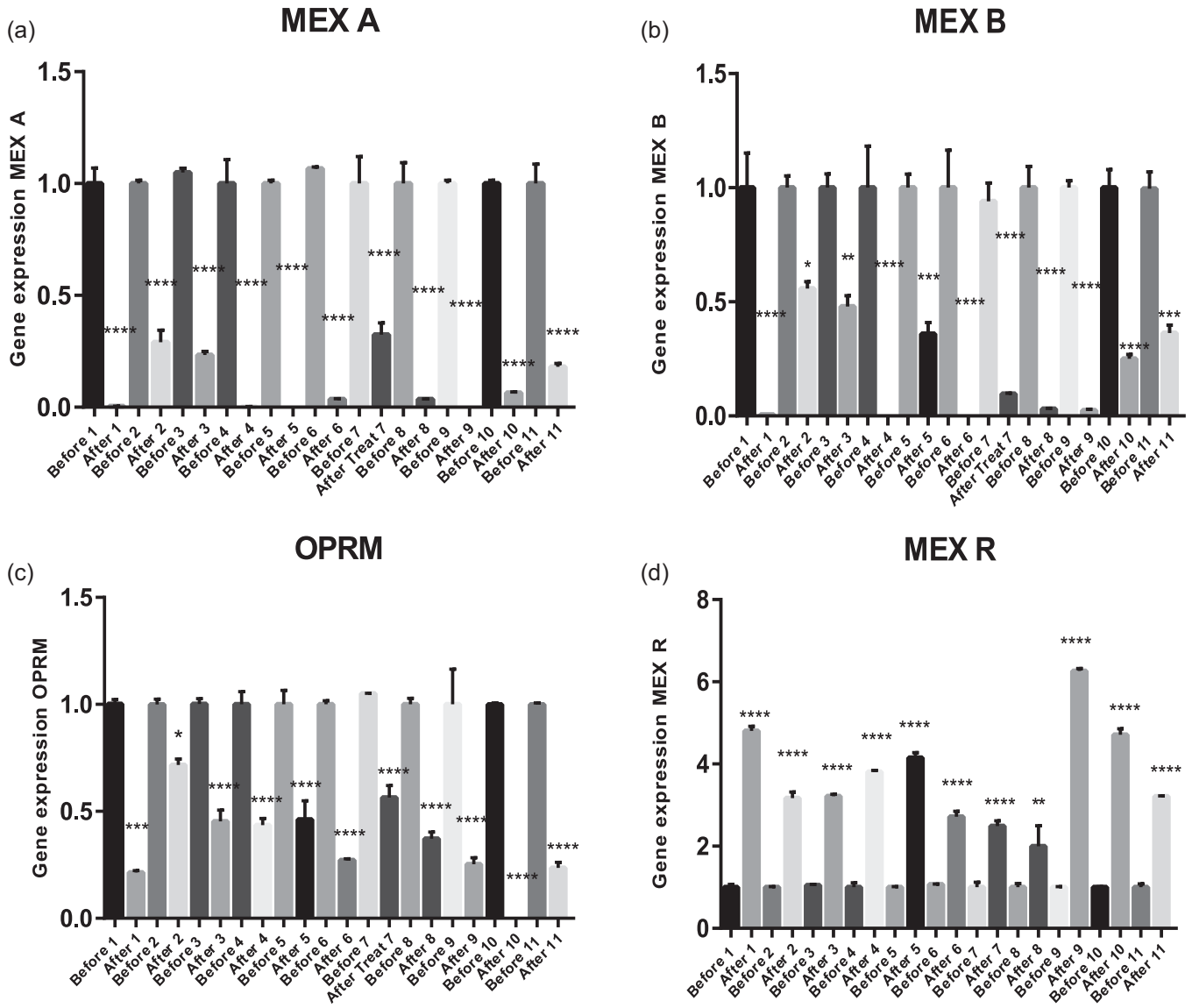

FIGURE 4 The expression rates of the *MexAB-oprM* efflux pump genes in the CuO nanoparticles-treated and nontreated isolates; a significant decrease was observed in gene expression; strain number 11 was the standard strain (ATCC: 27853); Relative fold change of the gene expression of (a) *mexA*, (b) *mexB*, (c) *oprM*, and (d) *mexR*.

CuO NPs utilizing MIC results [39]. In line with our study, it was showed antibacterial activity of carboxyl and amine groups on the bacterial cell surface could possibly attract Cu^{+2} ions toward the cell and confirmed antibacterial activity of CuO NPs which was consistent with our results [40–42]. Regarding these studies, CuO NPs can have significant antibacterial properties, which is consistent with our results.

The *mexA*, *mexB*, and *oprM* genes were down-regulated through the *mexR* overexpression as a known inhibitor of the mentioned genes, which proved the efficacy of the cited NPs. Similar to the results obtained from our study, Gholamrezazadeh et al. also showed that CuO NPs can down-regulate the biofilm genes of *Pseudomonas* bacteria [43]. Askarinia et al. observed a significant downexpression of *mecA* genes in clinical strains of *Staphylococcus aureus* after treatment with the synthesized NPs [44]. Sharifi et al. found that NPs had a weak inhibitory effect on the *mexA* expression in *P. aeruginosa* [25]. Moreover, silver NPs downregulated the *mexA* and *mexB* genes that results of the above two studies are consistent with our results [45]. Ahmed et al. also understood that the synthesized NPs reduced the expression of *P. aeruginosa* efflux pump genes [46]. Mahdi et al. observed the inhibitory effects of chitosan NPs on the *mexB* gene of *Pseudomonas* [47].

On the other hand, based on our results, the synthesized CuO NPs had a lethal dose-dependent

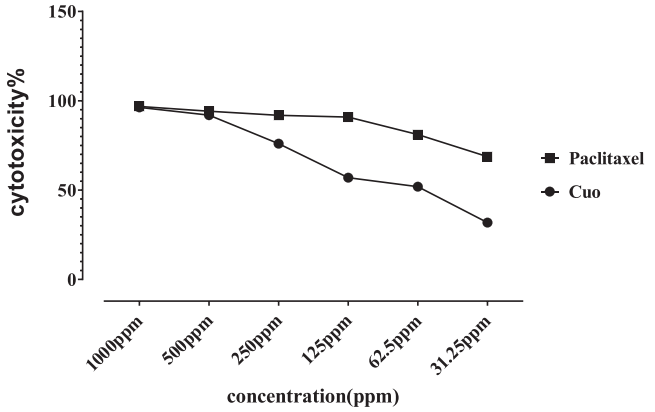

FIGURE 5 Comparison of cytotoxicity of nanoparticles (NPs) and taxol (with decreasing NPs and drug concentrations, cytotoxicity should be reduced).

activity against cancer cell. Furthermore, a study showed that CuO growth inhibition on the MCF7 cell line at different concentrations was higher than that of the AMJ13 breast cancer cell line. It also reported that cancer cells are more sensitive to CuO NPs than normal cells, which means CuO NPs have selective effects on cells [48]. Farhangi et al. also showed the cytotoxic effect of synthetic CuO NPs on MCF7 cell line in a dose-dependent manner with the least effect on normal cells [49]. In agreement with our observation, Thamer et al. reported cell growth inhibition of CuO NPs on the MCF7 cell line was dose-dependent [48]. Jeronsia et al. reported the cytotoxic effects of CuO NPs on the MCF7 cell line, too [50]. In contrast to our results Khatami et al. reported that 30 μg/mL of IC50 for silver NPs on MCF7 cell line which was higher than our IC50 (25.73 μg/mL), which can indicate that CuO NP is more effective than silver NPs. It can be due to a longer shelf life of Nanosized CuO than other organic antimicrobials, such as silver and gold [51]. So depending on the NP type, their effective concentration is different [52]. However, in a study, lower effective CuO NPs concentrations (IC50 = 20 μg/mL) on MCf7 cells was obtained compared with that of our research, which can be due to different production methods of NPs [53].

Understanding the behavior of NPs in real systems and their possible interactions with biological systems is crucial for the safe implementation of these materials in medical diagnostics and therapy [54]. Recent research showed that CuO NPs induce changes in lipid profile, oxidative stress, renal dysfunction, and etc in vivo under toxic conditions [55]. Numerous factors affect the inhibition of cancer cell lines, such as cell line type, treatment duration, the concentration of used treatment, and so forth. Growth inhibitory effect of NPs on cancer cells

TABLE 3 Results of CuO nanoparticles and taxol cytotoxicity.

Group												
CuO						Taxol						*p* Value
ppm	1000	500	250	125	62.5	31.25	1000	500	250	125	62.5	31.25	
	96.337 ± 1.540	91.950 ± 0.338	75.978 ± 0.965	56.94 ± 2.11	51.96 ± 2.69	31.85 ± 4.47	96.89 ± 1.79	94.165 ± 0.749	91.865 ± 0.484	90.885 ± 0.656	81.09 ± 1.97	68.738 ± 0.992	<0.0001

depends on the NPs morphology, size, and surface as well as cancer cell line type [56].

In summary, as antibiotic resistance is a huge threat to humanity and a large issue in medicine, introducing new materials with antibacterial activity and novel strategies that change antibiotic administration can be promising. The results of this study showed antibacterial properties and cytotoxic effects of CuO NPs as well as encouraged CuO NPs biosynthesis by the green method via *B. subtilis*. On the other hand, the antibacterial effect of CuO NPs was confirmed through the expression of *mexAB-oprM* output pump genes in *P. aeruginosa*. The evidence of this study demonstrated the application of nanotechnology in solving antibiotic resistance problems in human infections with *P. aeruginosa*. However, more laboratory studies are needed in terms of stability, surface modification, coating, and toxicity of CuO NPs on human cells and tissues.

ACKNWLEDGMENTS

We sincerely thank the directorator and staff of the Razi Herbal Medicines Research Center who assisted us.

CONFLICT OF INTEREST STATEMENT

The authors declare no conflict of interest.

DATA AVAILABILITY STATEMENT

The data that support the findings of this study are available from the corresponding author upon reasonable request.

ORCID

Neda Akbari http://orcid.org/0000-0003-4029-8756

REFERENCES

[1] Rachel R, Klingl A, Neuner C, Depmeier W, Schmalz G, Thomm M, editors, et al. Surface layers of ore-leaching Bacteria and Archaea. In: EMC 2008 14th European Microscopy Congress 1-5, September, Aachen, Germany; 2008, Springer; 137–8.

[2] Sadeghi da. Antimicrobial activity of *Ephedra pachyclada* methanol extract on some enteric Gram-negative bacteria which causes nosocomial infections by agar dilution method. Zahedan j res med sci. 2016;18(11):4015.

[3] Sharma NC, Sahi SV, Nath S, Parsons JG, Gardea-Torresde JL, Pal T. Synthesis of plant-mediated gold nanoparticles and catalytic role of biomatrix-embedded nanomaterials. Environ Sci Technol. 2007;41(14):5137–42.

[4] Shahbandeh M, Taati Moghadam M, Mirnejad R, Mirkalantari S, Mirzaei M. The efficacy of $AgNO_3$ nanoparticles alone and conjugated with imipenem for combating extensively drug-resistant *Pseudomonas aeruginosa*. Int J Nanomedicine. 2020;15:6905–16.

[5] Shariati A, Asadian E, Fallah F, Azimi T, Hashemi A, Yasbolaghi Sharahi J, et al. Evaluation of nano-curcumin effects on expression levels of virulence genes and biofilm production of multidrug-resistant *Pseudomonas aeruginosa* isolated from burn wound infection in Tehran, Iran. Infect Drug Resist. 2019;12:2223–35.

[6] Behoftadeh F, Faezi Ghasemi M, Mojtahedi A, Issazadeh K, Golshekan M, Alaei S. Development of a newly designed biosensor using multi-walled carbon nanotubes (MWCNTs) with gold nanoparticles (AuNPs) in the presence of acetaminophen for detection of *Escherichia coli*. Arch Microbiol. 2023;205(2):70.

[7] Amirpoor Z, Doudi M, Amiri GR. Biosynthesis of copper nanoparticles by *Stenotrophomonas maltophilia*. World J Microbiol. 2018;11(1):73–87.

[8] Nabila MI, Kannabiran K. Biosynthesis, characterization and antibacterial activity of copper oxide nanoparticles (CuO NPs) from actinomycetes. Biocatal Agric Biotechnol. 2018;15: 56–62.

[9] Hedayati Ch M, Mehmandoost Du E, Golshekan M, Mojtahedi A, Mobayen M. Synthesis of MCM-41@ SO_3H-polymixin B nanocomposite for extraction and determination of lipopolysaccharide from aqueous solutions using taguchi fractional factorial design. ChemistrySelect. 2022;7(45):e202203401.

[10] Shahbazi S, Shivaee A, Nasiri M, Mirshekar M, Sabzi S, Sariani OK Zinc oxide nanoparticles impact the expression of the genes involved in toxin–antitoxin systems in multidrug-resistant *Acinetobacter baumannii*. J Basic Microbiol. (2022).

[11] Ren G, Hu D, Cheng EWC, Vargas-Reus MA, Reip P, Allaker RP. Characterisation of copper oxide nanoparticles for antimicrobial applications. Int J Antimicrob Ag. 2009;33(6):587–90.

[12] Raffi M, Mehrwan S, Bhatti TM, Akhter JI, Hameed A, Yawar W, et al. Investigations into the antibacterial behavior of copper nanoparticles against *Escherichia coli*. Ann Microbiol. 2010;60(1):75–80.

[13] Lee HJ, Song JY, Kim BS. Biological synthesis of copper nanoparticles using *Magnolia kobus* leaf extract and their antibacterial activity. J Chem Technol Biotechnol. 2013;88(11):1971–7.

[14] Hoseinzadeh E, Alikhani M-Y, Samarghandi M-R, Shirzad-Siboni M. Antimicrobial potential of synthesized zinc oxide nanoparticles against Gram positive and Gram negative bacteria. Desalin Water Treat. 2014;52(25–27):4969–76.

[15] Stoimenov PK, Klinger RL, Marchin GL, Klabunde KJ. Metal oxide nanoparticles as bactericidal agents. Langmuir. 2002;18(17):6679–86.

[16] Singh S, Vidyarthi AS, Nigam VK, Dev A. Extracellular facile biosynthesis, characterization and stability of gold nanoparticles by *Bacillus licheniformis*. Artif Cells Nanomed Biotechnol. 2014;42(1):6–12.

[17] Nakhaeepour Z, Mashreghi M, Nakhaei Pour A, Moghaddam, Matin M, editors. Luminescent *Vibrio fischeri* as a platform for biosynthesis of cuo nanoparticles. Iran J Microbiol. 2017.

[18] Taati Moghadam M, Mirzaei M, Fazel Tehrani Moghaddam M, Babakhani S, Yeganeh O, Asgharzadeh S, et al. The challenge of global emergence of novel colistin-resistant *Escherichia coli* ST131. Microb Drug Resist. 2021;27(11):1513–24.

[19] Goodarzi NN, Fereshteh S, Sabzi S, Shahbazi S, Badmasti F. Construction of a chimeric FliC including epitopes of OmpA and OmpK36 as a multi-epitope vaccine against *Klebsiella pneumonia*. Heath Biotechnol. Biopharma. 2021;5:44–60.
[20] Moghadam MT, Shariati A, Mirkalantari S, Karmostaji A. The complex genetic region conferring transferable antibiotic resistance in multidrug-resistant and extremely drug-resistant *Klebsiella pneumoniae* clinical isolates. New Microbes New Infect. 2020;36:100693.
[21] Dimopoulos G, Akova M, Rello J, Poulakou G. Understanding resistance in *Pseudomonas*. Intensive Care Med. 2020;46(2):350–2.
[22] Qin S, Xiao W, Zhou C, Pu Q, Deng X, Lan L, et al. *Pseudomonas aeruginosa*: pathogenesis, virulence factors, antibiotic resistance, interaction with host, technology advances and emerging therapeutics. Signal Transduct Target Ther. 2022;7(1):199.
[23] Fujiwara M, Yamasaki S, Morita Y, Nishino K. Evaluation of efflux pump inhibitors of MexAB-or MexXY-OprM in *Pseudomonas aeruginosa* using nucleic acid dyes. J Infect Chemother. 2022;28(5):595–601.
[24] Ruiz-Roldán L, Rojo-Bezares B, de Toro M, López M, Toledano P, Lozano C, et al. Antimicrobial resistance and virulence of Pseudomonas spp. among healthy animals: concern about exolysin ExlA detection. Sci Rep. 2020;10(1):11667.
[25] Sharif R, Amini K. Effect of iron oxide nanoparticles and probiotic *Bifidobacterium bifidum* on MexA gene expression in drug resistant isolates of *Pseudomonas aeruginosa*. J Res Med Sci. 2019;43(3):118–23.
[26] Goli HR, Nahaei MR, Rezaee MA, Hasani A, Samadi Kafil H, Aghazadeh M, et al. Contribution of mexAB-oprM and mexXY (-oprA) efflux operons in antibiotic resistance of clinical *Pseudomonas aeruginosa* isolates in Tabriz, Iran. Infect Genet Evol. 2016;45:75–82.
[27] Al-Ahmadi GJ, Roodsari RZ. Fast and specific detection of *Pseudomonas aeruginosa* from other pseudomonas species by PCR. Ann Burns Fire Disasters. 2016;29(4):264.
[28] Weinstein MP, Lewis JS. The clinical and laboratory standards institute subcommittee on antimicrobial susceptibility testing: background, organization, functions, and processes. J Clin Microbiol. 2020;58(3):e01864–19.
[29] Wayne P. Reference method for broth dilution antifungal susceptibility testing of yeasts, approved standard. CLSI document M27-A2. 2002.
[30] Pourakbari B, Yaslianifard S, Yaslianifard S, Mahmoudi S, Keshavarz-Valian S, Mamishi S. Evaluation of efflux pumps gene expression in resistant *Pseudomonas aeruginosa* isolates in an Iranian referral hospital. Iran J Microbiol. 2016;8(4):249–56.
[31] Kim JB, Yu J-H, Ko E, Lee K-W, Song AK, Park SY, et al. The alkaloid Berberine inhibits the growth of Anoikis-resistant MCF-7 and MDA-MB-231 breast cancer cell lines by inducing cell cycle arrest. Phytomedicine. 2010;17(6):436–40.
[32] Sivaraj R, Rahman PKSM, Rajiv P, Narendhran S, Venckatesh R. Biosynthesis and characterization of *Acalypha indica* mediated copper oxide nanoparticles and evaluation of its antimicrobial and anticancer activity. Spectrochim Acta A Mol. 2014;129:255–8.
[33] Lahiri D, Nag M, Sheikh HI, Sarkar T, Edinur HA, Pati S, et al. Microbiologically-synthesized nanoparticles and their role in silencing the biofilm signaling cascade. Front Microbiol. 2021;12:180.
[34] Sutradhar P, Saha M, Maiti D. Microwave synthesis of copper oxide nanoparticles using tea leaf and coffee powder extracts and its antibacterial activity. J Nanostructure Chem. 2014;4(1):86.
[35] Shantkriti S, Rani P. Biological synthesis of copper nanoparticles using *Pseudomonas fluorescens*. Int J Curr Microbiol App Sci. 2014;3(9):374–83.
[36] Eltarahony M, Zaki S, Abd-El-Haleem D. Concurrent synthesis of zero-and one-dimensional, spherical, rod-, needle-, and wire-shaped CuO nanoparticles by *Proteus mirabilis* 10B. J Nanomater. 2018;3:1-14.
[37] Hansen LH, Johannesen E, Burmølle M, Sørensen AH, Sørensen SJ. Plasmid-encoded multidrug efflux pump conferring resistance to olaquindox in *Escherichia coli*. Antimicrob Agents Chemother. 2004;48(9):3332–7.
[38] Shahbazi S, Sabzi S, Noori Goodarzi N, Fereshteh S, Bolourchi N, Mirzaie B, et al. Identification of novel putative immunogenic targets and construction of a multi-epitope vaccine against multidrug-resistant *Corynebacterium jeikeium* using reverse vaccinology approach. Microb Pathog. 2022;164:105425.
[39] Ghasemian E, Naghoni A, Rahvar H, Kialha M, Tabaraie B. Evaluating the effect of copper nanoparticles in inhibiting *Pseudomonas aeruginosa* and Listeria monocytogenes biofilm formation. Jundishapur J Microbiol. 2015;8(5):17430.
[40] Chang Y-N, Zhang M, Xia L, Zhang J, Xing G. The toxic effects and mechanisms of CuO and ZnO nanoparticles. Materials. 2012;5(12):2850–71.
[41] Singh J, Vishwakarma K, Ramawat N, Rai P, Singh VK, Mishra RK, et al. Nanomaterials and microbes' interactions: a contemporary overview. 3 Biotech. 2019;9(3):1–14.
[42] Kim JS, Kuk E, Yu KN, Kim J-H, Park SJ, Lee HJ, et al. Antimicrobial effects of silver nanoparticles. Nanotechnol Biol Med. 2007;3(1):95–101.
[43] Gholamrezazadeh M, Shakibaie MR, Monirzadeh F, Masoumi S, Hashemizadeh Z. Effect of nano-silver, nano-copper, deconex and benzalkonium chloride on biofilm formation and expression of transcription regulatory quorum sensing gene (rh1R) in drug-resistance *Pseudomonas aeruginosa* burn isolates. Burns. 2018;44(3):700–8.
[44] Askarinia M, Ghaedi M, Manzouri L, Khoramrooz SS, Sharifi A, Ghalamfarsa G, et al. The effect of Cu-BPDCA-Ty on antibacterial activity and the expression of mecA gene in clinical and standard strains of methicillin-resistant *Staphylococcus aureus*. Jundishapur J Microbiol. 2018;11(3):e60680.
[45] Abdolhosseini M, Zamani H, Salehzadeh A. Synergistic antimicrobial potential of ciprofloxacin with silver nanoparticles conjugated to thiosemicarbazide against ciprofloxacin resistant *Pseudomonas aeruginosa* by attenuation of MexA-B efflux pump genes. Biologia. 2019;74(9):1191–6.
[46] Ahmed FY, Aly UF, Abd el-Baky RM, Waly NGFM. Effect of titanium dioxide nanoparticles on the expression of efflux pump and quorum-sensing genes in MDR *Pseudomonas aeruginosa* isolates. Antibiotics. 2021;10(6):625.

[47] Madhi M, Hasani A, Shahbazi Mojarrad J, Ahangarzadeh Rezaee M, Zarrini G, Davaran S, et al. Impact of Chitosan and silver nanoparticles laden with antibiotics on multidrug-resistant *Pseudomonas aeruginosa* and *Acinetobacter baumannii*. Arch Clin Infect Dis. 2020;15(4):100195.
[48] Thamer NA, Barakat NT, editors. Cytotoxic activity of green synthesis copper oxide nanoparticles using *Cordia myxa* L. aqueous extract on some breast cancer cell lines. J Phys Conf Ser; 2019.
[49] Javad Farhangi M, Es-Haghi A, Taghavizadeh Yazdi ME, Rahdar A, Baino F. MOF-mediated synthesis of CuO/CeO_2 composite nanoparticles: characterization and estimation of the cellular toxicity against breast cancer cell line (MCF-7). J Funct Biomater. 2021;12(4):53.
[50] Jeronsia J, Vidhya Raj D, Joseph L, Rubini K, Das S. In vitro antibacterial and anticancer activity of copper oxide nanostructures in human breast cancer Michigan cancer Foundation-7 cells. J Med Sci. 2016;36(4):145.
[51] Ijaz F, Shahid S, Khan SA, Ahmad W, Zaman S. Green synthesis of copper oxide nanoparticles using *Abutilon indicum* leaf extract: antimicrobial, antioxidant and photocatalytic dye degradation activitie. Trop J Pharm Res. 2017;16(4):743–53.
[52] Khatami M, Kharazi S, Kishani Farahani Z, Azizi H, Augusto Lima Nobre M. The anti-cancer effect of octagon and spherical silver nanoparticles on MCF-7 breast cancer cell line. Tehran Univ Med J. 2017;75(1):72–6.
[53] Zughaibi TA, Mirza AA, Suhail M, Jabir NR, Zaidi SK, Wasi S, et al. Evaluation of anticancer potential of biogenic copper oxide nanoparticles (CuO NPs) against breast cancer. J Nanomater. 2022;6:1–7.
[54] Sironmani A, Daniel K. Silver nanoparticles–universal multifunctional nanoparticles for bio sensing, imaging for diagnostics and targeted drug delivery for therapeutic applications. *Drug Dev Res*. 2011:463–84.
[55] Hosseini M-J, Shaki F, Ghazi-Khansari M, Pourahmad J. Toxicity of copper on isolated liver mitochondria: impairment at complexes I, II, and IV leads to increased ROS production. Cell Biochem Biophys. 2014;70(1):367–81.
[56] Wolfram J, Ferrari M. Clinical cancer nanomedicine. Nano Today. 2019;25:85–98.

How to cite this article: Azizi H, Akbari N, Kheirandish F, Sepahvand A. Biogenic synthesized copper oxide nanoparticles by *Bacillus subtilis*: Investigating antibacterial activity on the *mexAB-oprM* efflux pump genes and cytotoxic effect on MCF-7 cells. J Basic Microbiol. 2023;63:960–970. https://doi.org/10.1002/jobm.202200718